Fabrication and Characterization of Cast Magnesium Matrix Composites by Vacuum Stir Casting Process

Manchang Gui, Jianmin Han, and Peiyong Li

(Submitted 18 October 2002)

A vacuum stir casting process is developed to produce SiC_p reinforced cast magnesium matrix composites. This process can eliminate the entrapment of external gas onto melt and oxidation of magnesium during stirring synthesis. Two composites with Mg-Al9Zn and Mg-Zn5Zr alloys as matrices and 15 vol.% SiC particles as reinforcement are obtained. The microstructure and mechanical properties of the composites and the unreinforced alloys in as-cast and heat treatment conditions are analyzed and evaluated. In 15 vol.% SiC_p reinforced Mg-Al9Zn alloy-based composite (Mg-Al9Zn/15SiC_p), SiC particles distribute homogenously in the matrix and are well bonded with magnesium. In 15 vol.% SiC_p reinforced Mg-Zn5Zr alloy-based composite (Mg-Zn5Zr/15SiC_p), some agglomerations of SiC particles can be seen in the microstructure. In the same stirring process conditions, SiC reinforcement is more easily wetted by magnesium in the Mg-Al9Zn melt than in the Mg-Zn5Zr melt. The significant improvement in yield strength and elastic modulus for two composites has been achieved, especially for the Mg-Al9Zn/15SiC_p composite in which yield strength and elastic modulus increase 112 and 33%, respectively, over the unreinforced alloy, and increase 24 and 21%, respectively, for the Mg-Zn5Zr/15SiC_p composite. The strain-hardening behaviors of the two composites and their matrix alloys were analyzed based on the microstructure characteristics of the materials.

Keywords composite materials, magnesium alloy, microstructure, stir casting process, tensile properties

1. Introduction

Magnesium alloys are the lightest metallic structural materials. Magnesium (pure magnesium or its alloys) matrix composites maintain the low density of magnesium alloys. Furthermore, they possess higher strength and stiffness at room and elevated temperatures, and superior wear resistance and damping capacity.[1-5] Therefore, the composites have been considered an attractive choice for higher performance applications in the aerospace and automotive fields.

Magnesium matrix composites have been produced by different methods, such as stir casting,[1-4,6-10] powder metallurgy,[10-12] and squeeze casting.[5,13-15] Among these methods, stir casting would be considered an easily adaptable and most used method. An additional benefit of this process is the near-net-shape formation of the composites by conventional foundry processes. To avoid burning of molten magnesium alloy, the stir casting process for mixing reinforcement particles with the melt has been carried out under CO_2/SF_6 or inert Ar protective atmosphere. Due to vortex, these protective gases could be engulfed into the melt during stir casting, thereby causing higher porosity in the obtained composite.[1] Saravanan et al.[3] developed a casting process for the synthesis of particle reinforced Mg matrix composites without the use of flux and protective gas atmosphere. The process does not eliminate, however, the oxidation possibility of magnesium melt due to the existence of oxidation atmosphere above the melt surface. In comparison with aluminum matrix composites, the research and development of magnesium matrix composites are still limited. A key reason is perhaps related to the difficulty in synthesizing Mg matrix composites due to the high chemical activity of elemental Mg. The objective of the present study is to develop a stir casting process to fabricate SiC_p reinforced cast magnesium matrix composites under vacuum condition. The microstructure and mechanical properties of the as-cast composite materials are investigated, and the same work is also performed for the unreinforced magnesium alloys to compare them with the composites.

Manchang Gui and **Peiyong Li**, National Laboratory of Advanced Composites, Institute of Aeronautical Materials, Beijing, 100095, China; and **Jianmin Han,** Mechanical and Electrical College, Northern Jiaotong University, Beijing, 100044, China. Contact e-mail: manchangg@hotmail.com.

2. Experimental Procedures

Magnesium matrix composites reinforced with 15 vol.% SiC_p were produced by the stir casting process in vacuum condition. Commercial Mg-Al9Zn (AZ91C) and Mg-Zn5Zr (ZK51A) alloys were used as the matrices. Their chemical compositions are listed in Table 1. The reinforcement particles are high purity SiC with an average size of 12.8 μm. SiC particles were dried at 250 °C for 3 h prior to addition on molten magnesium alloys.

Figure 1 shows the schematic diagram of the apparatus used for fabrication of Mg matrix composites. The apparatus consists of three systems: electrical resistant heating, evacuation, and stirring systems. The impeller made of stainless steel was driven with a direct current (DC) engine so that the stirring rate could be exactly controlled and measured. Two thermocouples were installed. One was used to control the temperature of the electric furnace and the other to measure the temperature of the melt. The whole process is as follows:

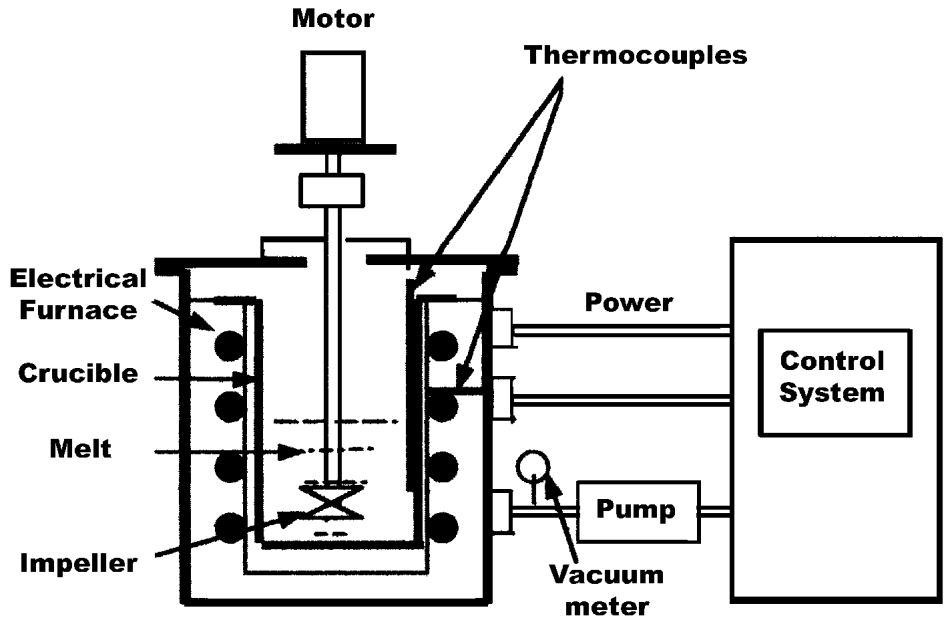

Fig. 1 Schematic diagram of the apparatus for fabrication of Mg matrix composites

Table 1 Chemical Compositions of Mg-Al9Zn and Mg-Zn5Zr Matrix Alloys

Element, wt%	Mg	Al	Zn	Mn	Zr	Cu	Si	Fe	Ni
Mg-Al9Zn	bal. (a)	8.60	0.52	0.36	…	<0.03	<0.03	<0.01	<0.05
Mg-Zn5Zr	bal.	…	4.54	…	0.68	<0.05	0.15	0.06	<0.01

(a) Bal., balance quantity

1) 1.5 kg magnesium alloy was charged in a steel crucible preheated at 400 °C in the electric furnace. The melt surface was covered with a flux salt to avoid burning of the magnesium alloy when the alloy was melted. At about 720 °C for the Mg-Al9Zn alloy and 740 °C for the Mg-Zn5Zr alloy, the melt was refined for 6-8 min by stirring it up and down with a skim ladle. The melt temperature was then decreased to about 700 °C.
2) After carefully cleaning the surface of the melt, all preheated SiC particles were quickly added onto the molten surface. A stirring part was put in place and the electric resistance furnace was evacuated to the level of 2-4 kPa. Then the mixing motor was turned on. The rotating rate of the steel impeller was gradually increased to about 1500 rpm. Stirring lasted about 25 min. Once the stirring began, the furnace temperature was regulated to 600 °C.
3) The motor was stopped. Argon was charged into the furnace and the impeller was removed. The composite melt was around 590-600 °C, and in a semisolid state at the end of the stirring process. The melt was heated to about 700 °C and poured into a permanent steel mold to form ingots of 215 × 45 × 22 mm.

The same ingots were also poured for the unreinforced magnesium alloys. The ingots were heat treated and then cut into specimens for tensile testing.

The densities of matrix alloys and composite materials were measured by a weight loss method using an electron balance with a resolution of 0.01 g. Porosity of the composites was estimated by the equation of $1 - \rho_m/\rho_{th}$, where ρ_m and ρ_{th} are the measured and theoretical densities, respectively. And, $\rho_{th} = \rho_{Mg}V_{Mg} + \rho_{SiC}V_{SiC}$, where ρ_{Mg} and ρ_{SiC} are the density of the matrix alloy and SiC, respectively (the measured density was taken for matrix and 3.2 $g \cdot cm^{-3}$ for SiC), and V_{Mg} and V_{SiC} are the volume fraction of matrix and SiC particles in the composites, respectively. The addition amount, 15 vol.%, was adapted for the volume fraction of SiC particles in the estimation.

A solution heat treatment (T4) was carried out for 18 h at 415 °C for Mg-Al9Zn alloy and Mg-Al9Zn/15SiC_p composite under CO_2 protective atmosphere. Aging treatment (T1) at 175 °C for 14 h without any solution treatment was performed for the Mg-Zn5Zr alloy and the Mg-Zn5Zr A/15SiC_p composite.

An optical microscope with an image analysis system was used to observe microstructure and measure the grain size, and the matrix/SiC interface was observed by using a scanning electron microscope (SEM). The tensile specimens were cut from the heat-treated ingots as the scheme indicated in Fig. 2(a). The size of tensile specimens is shown in Fig. 2(b). The tensile test was carried out at a strain rate of 8×10^{-3} s^{-1} using an MTS 810 machine equipped with a computer data acquisi-

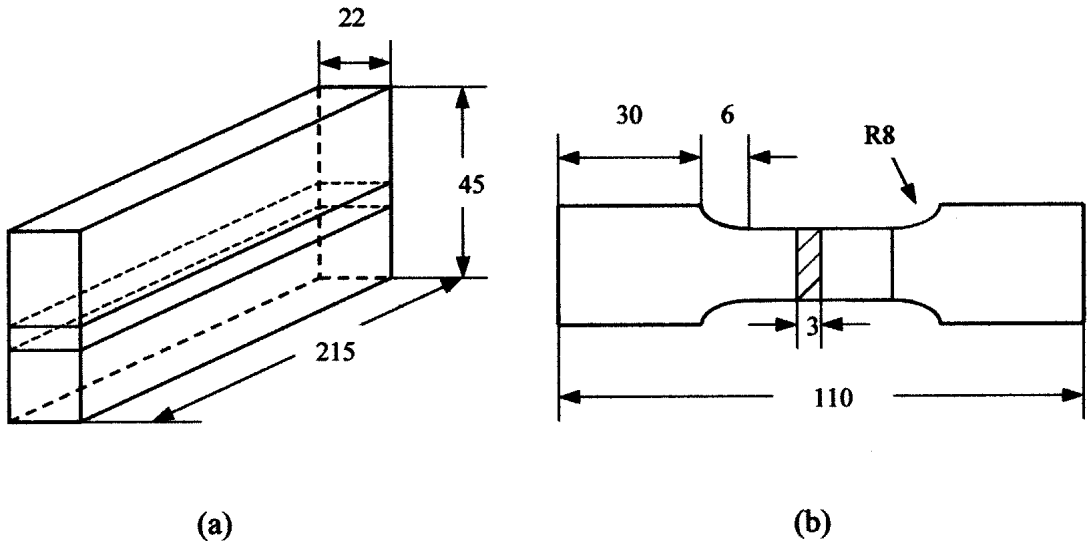

Fig. 2 Diagram of **(a)** the scheme of obtaining tensile specimen from ingots; **(b)** the size of plat tensile specimen

tion system, and with a gage length of 25 mm. The tensile property data were based on the average of four tests.

3. Results and Discussion

Visual inspection of cast and machined surfaces of two composite ingots showed that cast defects and macrosegregation of SiC particles were not noticed. No gas bubbles from engulfing external gas due to a vortex can be seen in the composite ingots. In the present process, the significant advantage is to eliminate the entrapment of external gas onto melt and oxidation of magnesium during the stirring synthesis. Table 2 gives the densities of matrix and composite ingots and the estimated porosity of the composites. It is found that the porosity of the Mg-Al9Zn/15SiC_p composite is markedly less than that of the Mg-Zn5Zr/15SiC_p composite, indicating that the Mg-Al9Zn/15SiC_p composite obtained by the present stir casting process possesses better metallurgical quality. Note that the high porosity in the Mg-Zn5Zr/15SiC_p composite does not result from the gas entrapment, which will be analyzed in the following context.

Figure 3 shows the optical microstructure of the Mg-Al9Zn alloy and its composite reinforced with 15 vol.% SiC_p in T4 heat treatment condition. Figure 4 shows the optical microstructure of the Mg-Zn5Zr alloy and its composite reinforced with 15 vol.% SiC_p at T1 heat treatment condition. From Fig. 3 and 4, Mg-Al9Zn and Mg-Zn5Zr alloys and their composites exhibit equiaxial grain structure with obscure grain boundaries. In the Mg-Al9Zn/15SiC_p composite, distribution of SiC particles is rather uniform, and SiC particles disperse in the matrix separately; no evident agglomeration of SiC particles can be found. On the basis of the microstructure in higher magnification (Fig. 3c) and the SEM photograph (Fig. 5), SiC particles are bonded with magnesium matrix intimately, and no evidence of significant chemical reaction between SiC/Mg interfaces is found. In addition, SiC particles are located at the grain boundaries as well as within the primary magnesium grains (Fig. 3c).

Table 2 Densities of Matrices and Composites and Porosity of Composites

Materials	Density, Mg · m^{-3}	Porosity, %
Mg-Al9Zn	1.795	…
Mg-Al9Zn/15SiC_p	1.984	1.1
Mg-Zn5Zr	1.804	…
Mg-Zn5Zr/15SiC_p	1.909	5.2

In the case of the Mg-Zn5Zr/15SiC_p composite, some agglomerations of SiC particles and pores enclosed by those SiC particles can be seen in the microstructure (Fig. 4b), thereby resulting in a low density of the composite ingot. The SiC particles in the agglomerations have not or have partially been bonded by magnesium matrix. The pores in the microstructure resulted neither from gas separation from the melt during solidification nor from entrapment of external gas into the melt during the stirring process. The initial SiC powders have not been dispersed completely to cause these agglomerations and pores. This phenomenon indicates that the wettability of SiC by magnesium in the Mg-Zn5Zr alloy melt is worse than that in the Mg-Al9Zn alloy melt in the same stirring process conditions. A reasonable explanation for the relatively poor wettability is that the aluminum alloying element is not contained in the Mg-Zn5Zr alloy, while aluminum in Mg alloys has proved to further improve the wettability because certain interfacial reactions occur by adding aluminum.[10] Certainly, it is probable to eliminate these SiC agglomerations by improving the parameters of the stirring process, such as stirring temperature and time, and further work on this aspect will be carried out. Figure 4(b) also demonstrates that the other SiC particles besides those in agglomerations are well dispersed in the magnesium matrix and are in intimate contact with the magnesium matrix. As with the Mg-Al9Zn/15SiC_p composite, SiC particles in the Mg-Zn5Zr/15SiC_p composite are segregated at the grain boundaries or entrapped within the primary magnesium grains (Fig. 4c).

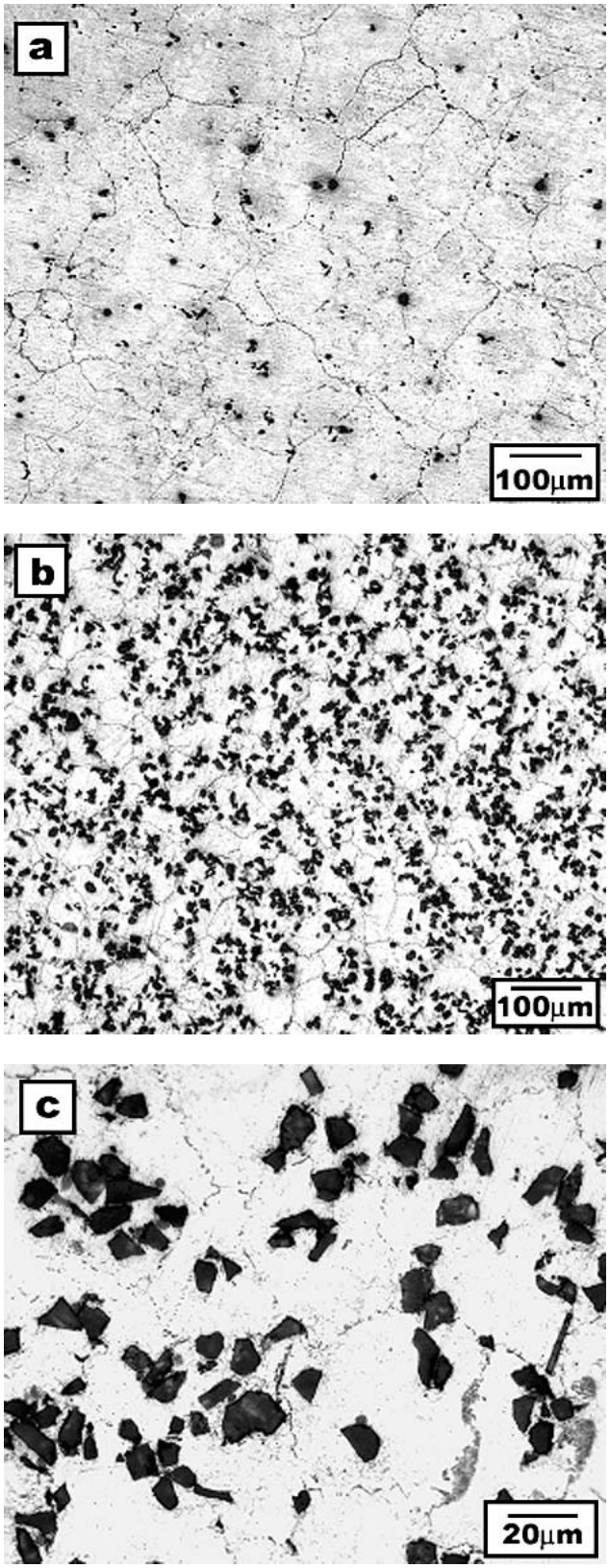

Fig. 3 Microstructure of Mg-Al9Zn alloy and Mg-Al9Zn/15SiC_p in T4 heat treatment condition. **(a)** Mg-Al9Zn alloy; **(b)** Mg-Al9Zn/15SiC_p composite; **(c)** higher magnification for Mg-Al9Zn/15SiC_p composite

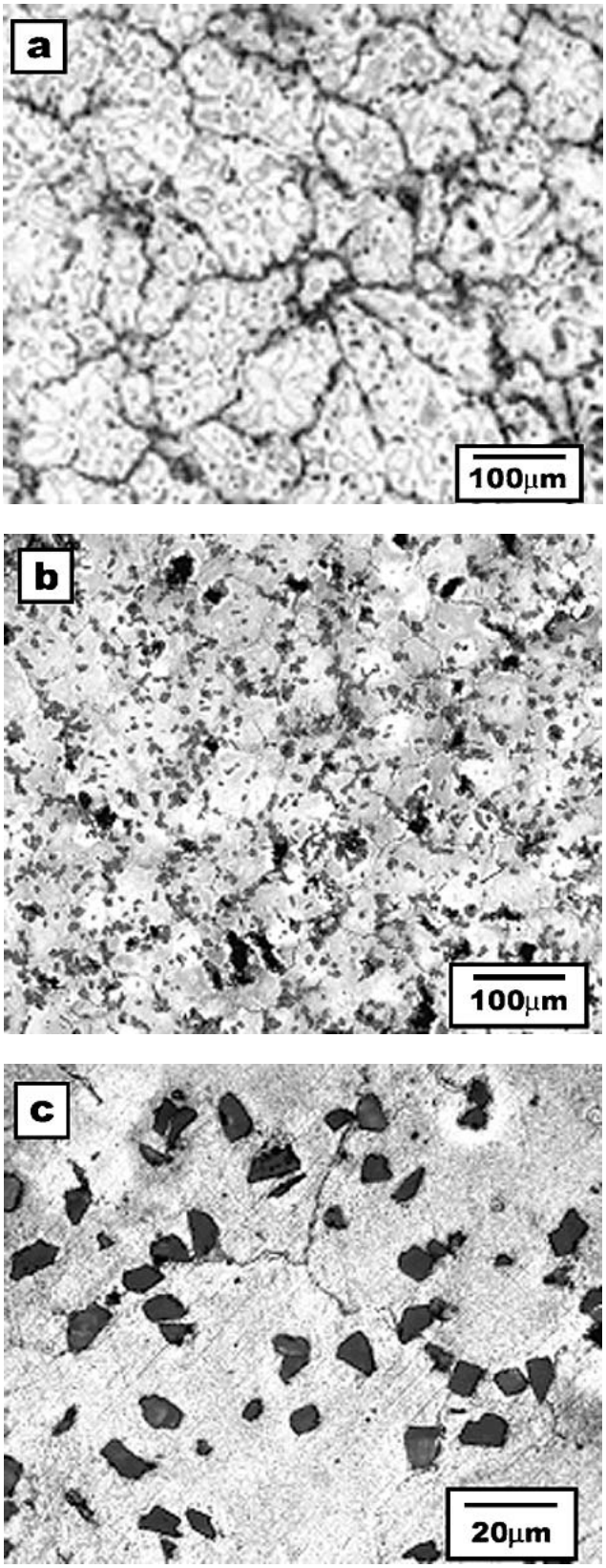

Fig. 4 Microstructure of Mg-Zn5Zr alloy and Mg-Zn5Zr/15SiC_p in T1 heat-treatment condition. **(a)** Mg-Zn5Zr alloy; **(b)** Mg-Zn5Zr/15SiC_p composite; **(c)** higher magnification for Mg-Zn5Zr/15SiC_p composite

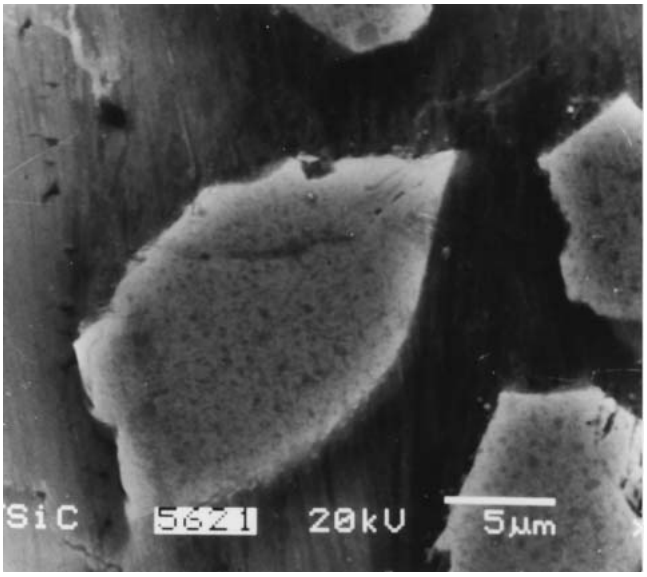

Fig. 5 SEM photograph showing the magnesium matrix/SiC interface

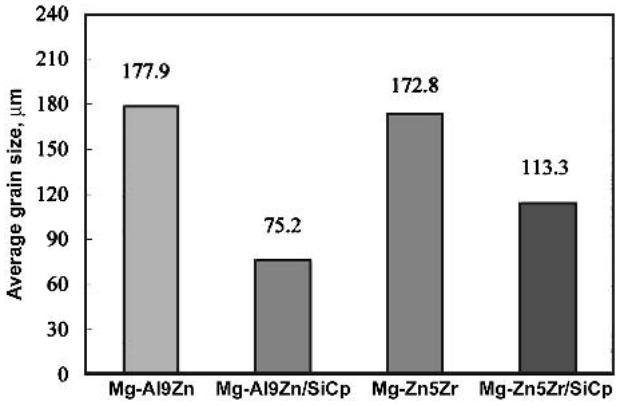

Fig. 6 Average grain sizes of the magnesium matrix composites and the corresponding matrix alloys

In addition, it is notable that the presence of SiC particles causes the refinement of magnesium grains. Figure 6 indicates the average grain sizes of two composites and their comparison with the unreinforced magnesium alloys in heat-treated conditions. The grain size of the matrix in the Mg-Al9Zn/15SiC$_p$ composite is reduced to 42% of that of the unreinforced Mg-Al9Zn alloy. The refinement effect in the Mg-Zn5Zr/15SiC$_p$ composite is not as much as that in the Mg-Al9Zn/15SiC$_p$ composite. The average grain size of the matrix magnesium grains in Mg-Zn5Zr/15SiC$_p$ decreases 35% due to the presence of SiC particles. The refinement mechanism has been reasonably characterized in some studies.[7-8,16-17] It has been reported that the grain refinement results from the heterogeneous nucleation of the primary magnesium phase on the surface of SiC particles with certain crystallographic orientation relationships and the restricted growth of magnesium crystals by SiC particles during solidification. Only SiC particles, which can act as the heterogeneous nucleation site, would be captured by growing magnesium crystals and finally stay within the magnesium grains in the composites.

The typical stress-strain curves of the as-cast Mg-Al9Zn alloy and the Mg-Al9Zn/15SiC$_p$ composite, and the Mg-Zn5Zr alloy and the Mg-Zn5Zr/15SiC$_p$ composite in heat-treated conditions are shown in Fig. 7. The tensile properties of all the as-cast materials obtained are given in Table 3. Because the tensile specimens were cut from thick ingots with low cooling rates, all materials exhibit relatively low ultimate tensile strength (UTS). The yield strengths of two composites are significantly higher (up to 112 and 24% for the Mg-Al9Zn/15SiC$_p$ and Mg-Zn5Zr/15SiC$_p$ composites, respectively) than the unreinforced magnesium alloys, and the UTS are slightly lower than those of the magnesium alloys. Meanwhile, the elastic modulus for two composites (up to 33% for Mg-Al9Zn/15SiC$_p$ and 21% for Mg-Zn5Zr/15SiC$_p$) increased significantly, which can directly be indicated from the higher slopes of the linear portion of the curves for the Mg-Al9Zn/15SiC$_p$ and Mg-Zn5Zr/15SiC$_p$ composites than for the Mg-Al9Zn and Mg-Zn5Zr alloys in Fig. 7. However, the elongations of the Mg-Al9Zn/15SiC$_p$ and Mg-Zn5Zr/15SiC$_p$ composites are drastically decreased to 1.1 and 1.8%, respectively, compared with the 7.2 and 7.3% elongations of the unreinforced Mg-Al9Zn and Mg-Zn5Zr alloys, respectively. In the case of the Mg-Zn5Zr/15SiC$_p$ composite, some agglomerations of SiC particles have been observed in the microstructure (Fig. 4b), but its yield strength and elastic modulus still exhibit a certain increase. However, the increase in yield strength and elastic modulus for the Mg-Al9Zn/15SiC$_p$ composite is more significant than for the Mg-Zn5Zr/15SiC$_p$ composite due to more uniform distribution of SiC particles and the intimate bond between SiC particles and magnesium.

The strain-hardening behaviors of the two alloys and composites were investigated through the differentiation to the stress-strain curves in Fig. 7. The strain-hardening rates versus true plastic strains are shown in Fig. 8. From Fig. 8(a), it is found that the strain-hardening rate of the Mg-Al9Zn/15SiC$_p$ composite during plastic deformation is higher than that of the unreinforced Mg-Al9Zn alloy, while their difference decreases with increasing plastic deformation, and even the rates of the two materials almost become the same. However, as shown in Fig. 8(b), the change tendency in the strain-hardening behaviors of the Mg-Zn5Zr alloy and Mg-Zn5Zr/15SiC$_p$ composite is different from that of the above two materials. The rate of the Mg-Zn5Zr/15SiC$_p$ composite is higher first, and then lower than that of the Mg-Zn5Zr alloy, with the increasing plastic strain.

The strengthening effect achieved in the composites, i.e., the increases in yield strength and elastic modulus as compared with the unreinforced magnesium alloys, can be attributed to the presence of the hard SiC particles. SiC particles distributing within the magnesium grains and at primary magnesium boundaries highly constrain the slip behavior of the magnesium grains, because the particles with large elastic stiffness and fracture strength are too strong to be deformed. The barrier to slip in the magnesium matrices of SiC particles also cause the higher strain-hardening rates for the composites in the early stage of plastic deformation, because a greater load increment must be used if the same deformation is obtained as compared with the unreinforced magnesium alloys. From the evaluation

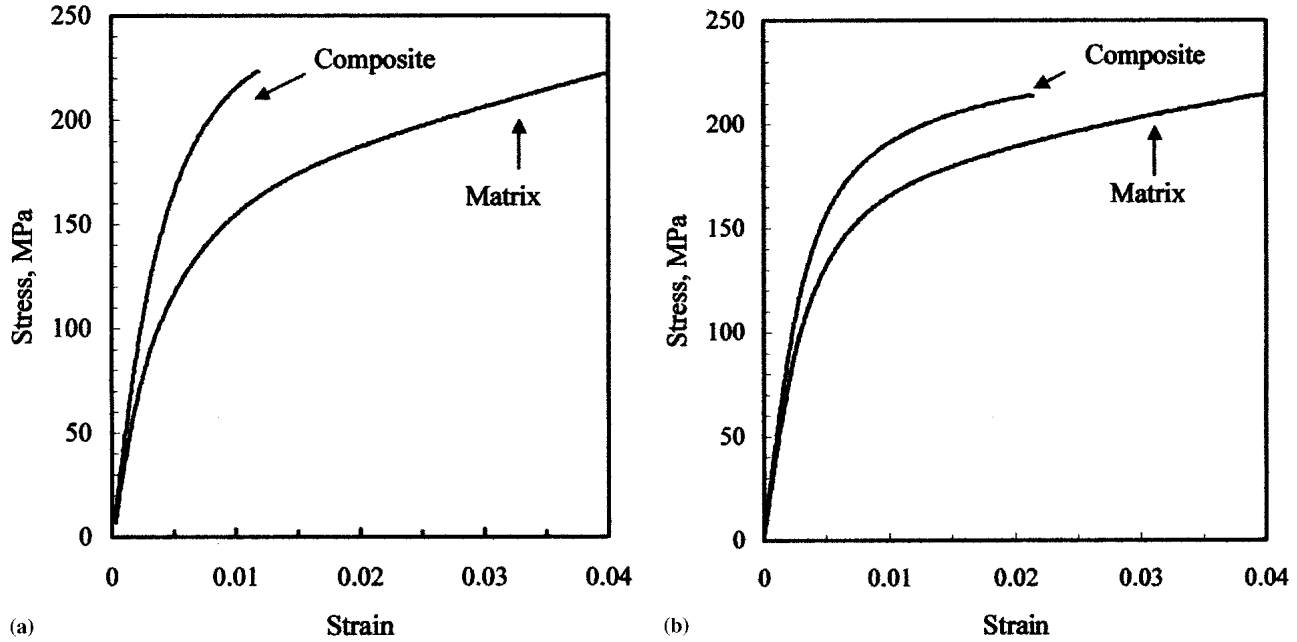

Fig. 7 Stress-strain curves for the unreinforced magnesium alloys and their composite. **(a)** Mg-Al9Zn alloy and Mg-Al9Zn/15SiC$_p$ composite; **(b)** Mg-Zn5Zr alloy and Mg-Zn5Zr/15SiC$_p$ composite

Table 3 Tensile Properties of the Two Matrix Alloys and Their Composites

Materials	Yield Strength, MPa	Tensile Strength, MPa	Elongation, %	Elastic Modulus, GPa
Mg-Al9Zn	84	225	7.2	42.7
Mg-Al9Zn/15SiC$_p$	178	218	1.1	57.0
Mg-Zn5Zr	131	221	7.3	43.2
Mg-Zn5Zr/15SiC$_p$	162	210	1.8	52.4

of grain sizes as shown in Fig. 6, significant grain refinement was achieved in the two composites, which should also contribute the strengthening of the composite materials. The grain boundary can act as a barrier to the slip process; therefore the increase in the grain boundary from magnesium grain refinement makes the deformation of magnesium grains more difficult.

Under an external load during the tensile test, a strong internal stress must develop between SiC particles and the matrix. The local stress concentration would be created due to the particle/matrix interaction, and localized damage may occur when the local stress is beyond the strength of the material at higher strain levels. As for composites, the localized damage could be in the forms of particle cracking, matrix cracking, and interface debonding.[18] Inclusion and particle agglomeration (if they exist) should also be the source of the localized damage. The localized damage can relax the internal stress and therefore decrease the strain-hardening rate for the composites. The final fracture of the composites results from the coalescence of the localized damages. In the present composites, SiC particles are distributed within the magnesium grains or at primary magnesium boundaries, which improve the uniformity of SiC particles. Further, the uniform distribution of SiC particles can improve the uniformity of stress distribution, thereby reducing or delaying the formation of localized damage. So the phenomenon of internal stress relaxation occurs rarely. As described above, the presence of SiC particles greatly constrains the slip behavior, therefore increasing the strain-hardening rates for the composites in the early stage of plastic deformation. Meanwhile, the localized damage is limited in the Mg-Al9Zn/15SiC$_p$ composite, and is absent in the unreinforced Mg-Al9Zn alloy. This results in the higher or similar strain-hardening rate for the Mg-Al9Zn/15SiC$_p$ composite over the unreinforced Mg-Al9Zn alloy in the whole plastic deformation of the composite. In the Mg-Zn5Zr/15SiC$_p$ composite, however, the localized damage exhibits differently due to the presence of SiC particle agglomerations and pores resulting from the agglomerations. These defects, in fact, are the crack source and will be propagated when the external load reaches a certain value, which causes serious localized damage. It can be proved from the tensile fracture of the composite where the SiC agglomerations were readily seen. Therefore, the internal stress relaxation from the localized damage will cause the decrease of the strain-hardening rate, resulting in a lower rate than that of the unreinforced Mg-Zn5Zr alloy after a certain plastic deformation.

4. Conclusions

1) The vacuum stir casting process is developed to produce SiC particle-reinforced Mg-Al9Zn and Mg-Zn5Zr cast magnesium matrix composites. No macrosegregation of SiC particles and gas bubbles can be found in the composite ingots. This process can eliminate the entrapment of exter-

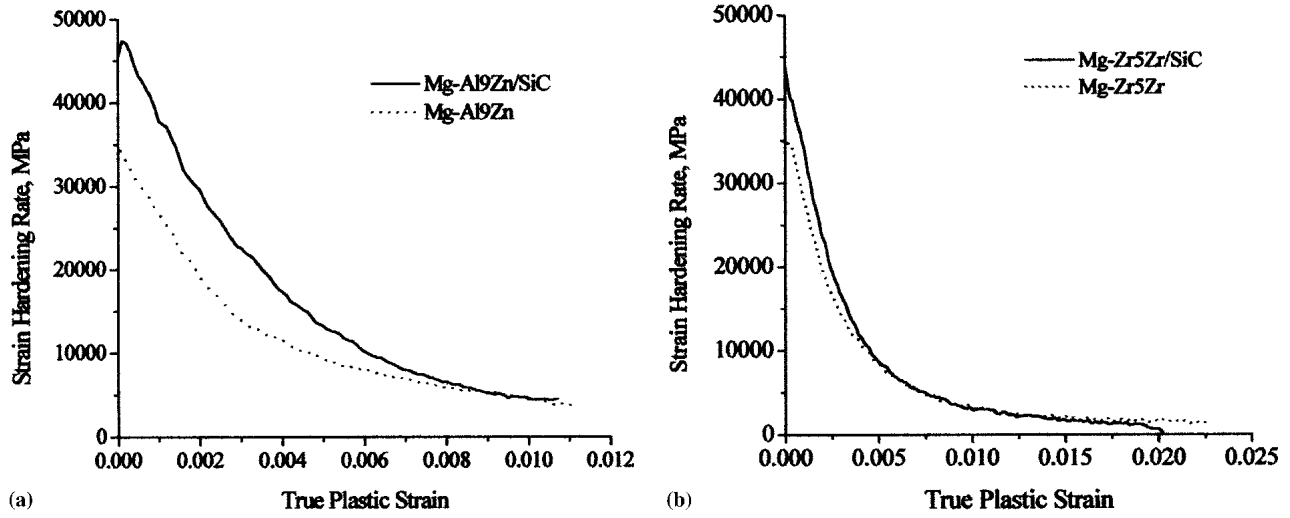

Fig. 8 Strain hardening rate vs true plastic strain curves for **(a)** unreinforced Mg-Al9Zn alloy and Mg-Al9ZnZn/SiC composite; **(b)** unreinforced Mg-Zn5Zr alloy and Mg-Zn5Zr/SiC composite

nal gas onto melt and oxidation of magnesium during stirring synthesis.

2) In the microstructure of the Mg-Al9Zn/15SiC$_p$ composite, SiC particles exhibit a reasonably homogenous distribution and SiC reinforcements are well bonded by magnesium. In the Mg-Zn5Zr/15SiC$_p$ composite, some agglomerations of SiC particles can be seen. At the same stirring process conditions, the wettability of SiC by magnesium in the Mg-Zn5Zr melt is worse than that in the Mg-Al9Zn melt.
3) Both composites exhibit significant improvement in yield strength and elastic modulus, especially for the Mg-Al9Zn/15SiC$_p$ composite. A 112% increase in yield strength and 33% increase in elastic modulus are obtained for this composite compared with the unreinforced magnesium alloy, while increases of 24 and 21%, respectively, were observed for theMg-Zn5Zr/15SiC$_p$ composite.

References

1. V. Laurent, P. Jarry, G. Regazzoni, and D. Apelian: "Processing-Microstructure Relationships in Compocast Magnesium/SiC," *J. Mater. Sci.,* 1992, *27,* pp. 4447-59.
2. A. Martin and J. Llorca: "Mechanical Behavior and Failure Mechanisms of a Binary Mg-6%Zn Alloy Reinforced With SiC Particulates," *Mater. Sci. Eng.,* 1995, *A201,* pp. 77-87.
3. R.A. Saravanan and M.K. Surappa: "Fabrication and Characterization of Pure Magnesium-30 Vol.% SiCp Particulate Composite," *Mater. Sci. Eng.,* 2000, *A276*, pp. 108-16.
4. S.C. Sharma, B. Anand, and M. Krishna: "Evaluation of Sliding Wear Behavior of Feldspar Particle-Reinforced Magnesium Alloy Composites," *Wear,* 2000, *241,* pp. 33-40.
5. C. Mayencourt and R. Schaller: "Mechanical-Stress Relaxation in Magnesium-Based Composites," *Mater. Sci. Eng.*. 2002, *A325*, pp. 286-91.
6. A. Bochenek and K.N. Braszczynska: "Structural Analysis of the MgAl5 Matrix Cast Composites Containing SiC Particles*," Mater. Sci. Eng.,* 2000, *290A,* pp. 122-27.
7. Y. Cai, M.J. Tan, G.J. Shen, and H.Q. Su: "Microstructure and Heterogeneous Nucleation Phenomena in Cast SiC Particles Reinforced Magnesium Composite*," Mater. Sci. Eng.,* 2000, *282A,* pp. 232-39.
8. H. Hu: "Grain Microstructure Evolution of Mg (AM50A)/SiCp Metal Matrix Composites," *Scripta Mater.,* 1998, *39,* pp. 1015-22.
9. T. Imai, S.W. Lim, D. Jiang, Y. Nishida, and T. Imura: "Superplasticity of Ceramic Particulate Reinforced Magnesium Alloy Composite Made by a Vortex Method," *Mater. Sci. Forum,* 1999, *304/306*, pp. 315-20.
10. A. Luo: "Processing, Microstructure, and Mechanical Behavior of Cast Magnesium Metal Matrix Composites," *Metall. Mater. Trans.,* 1995, *26A*, pp. 2445-55.
11. H. Ferkel and B.L. Mordike: "Magnesium Strengthened by SiC Nanoparticles," *Mater. Sci. Eng.,* 2001, *298,* pp. 193-99.
12. B.W. Chua, L. Lu, and M.O. Lai: "Influence of SiC Particles on Mechanical Properties of Mg Based Composite," *Compos. Struct.,* 1999, *47*, pp. 595-601.
13. M. Yoshida, S. Takeuchi, J. Pan, G. Sasaki, N. Fuyama, T. Fujii, and H. Fukunaga: "Preparation and Characterization of Aluminum Borate Whisker Reinforced Magnesium Alloy Composites by Semi-solid Process," *Adv. Compos. Mater.,* 1999, *8,* pp. 258-68.
14. L. Hu and E. Wang: "Fabrication and Mechanical Properties of SiCw/ZK51A Magnesium Matrix Composite by Two-step Squeeze Casting," *Mater. Sci. Eng.,* 2000, *278A,* pp. 267-71.
15. M.Y. Zheng, K. Wu, and C.K. Yao: "Effect of Interfacial Reaction on Mechanical Behavior of SiCw/AZ91 Magnesium Matrix Composites," *Mater. Sci. Eng.,* 2001, *318A,* pp. 50-56.
16. Y. Cai, D. Taplin, M.J. Tan, and W. Zhou: "Nucleation Phenomenon in SiC Particulate Reinforced Magnesium Composite," *Scripta Mater.,* 1999, *41,* pp. 967-71.
17. A. Luo: "Development of Matrix Grain Structure During the Solidification of an Mg (AZ91)/SiC$_p$ Composite," *Scripta Metall. Mater.,* 1994, *31,* pp. 1253-58.
18. P.M. Singh, and J.J. Lewandowki: "Effects of Heat Treatment and Reinforcement Size on Reinforcement Fracture During Tension Testing of a SiC$_p$ Discontinuously Reinforced Aluminum Alloy," *Metall. Trans. A,* 1993, *24A,* pp. 2531-43.